

Star Formation by Hierarchical Gravitational Collapse



UNIVERSIDAD NACIONAL
AUTÓNOMA DE MÉXICO

Enrique Vázquez-Semadeni

Centro de Radioastronomía y Astrofísica, UNAM



Collaborators:

CRyA UNAM:

Gilberto Gómez

Pedro Colín

Javier Ballesteros-
Paredes.

ABROAD:

Katharina Jappsen (Cardiff)

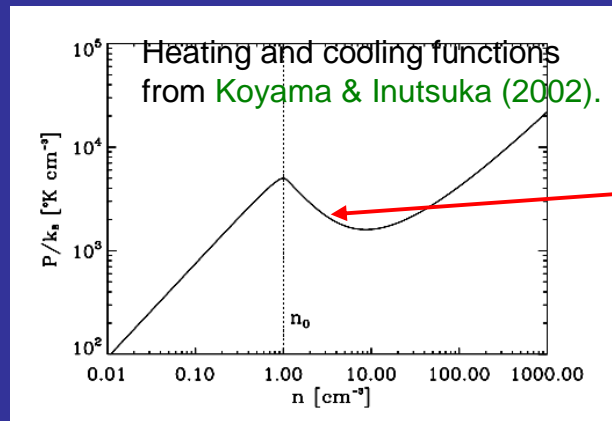
Ralf Klessen (ITA Heidelberg)

I. Introduction

- High-mass star-forming cores are systematically denser, more massive and more “turbulent” (have higher velocity dispersions) than low-mass star-forming cores (e.g., Garay & Lizano 1999; Kurtz et al. 2000; Beuther et al. 2007).
- Recent work has proposed that GMCs and clumps may be in a generalized process of gravitational contraction (Burkert & Hartmann 2004; Hartmann & Burkert 2007; VS et al. 2007; Peretto et al. 2007).
- This talk:
 - Present recent results (Vázquez-Semadeni et al. 2009, ApJ, 707, 1023) suggesting that
 - low-mass star-forming regions result from local, small-scale collapse in GMCs.
 - high-mass star-forming regions are the culmination of the global collapse of a GMC.
 - These trends continue even in the presence of stellar feedback (Vázquez-Semadeni et al. 2010, ApJ, 715, 1302).

II. Search for massive-SF-like regions in numerical simulations of MC formation

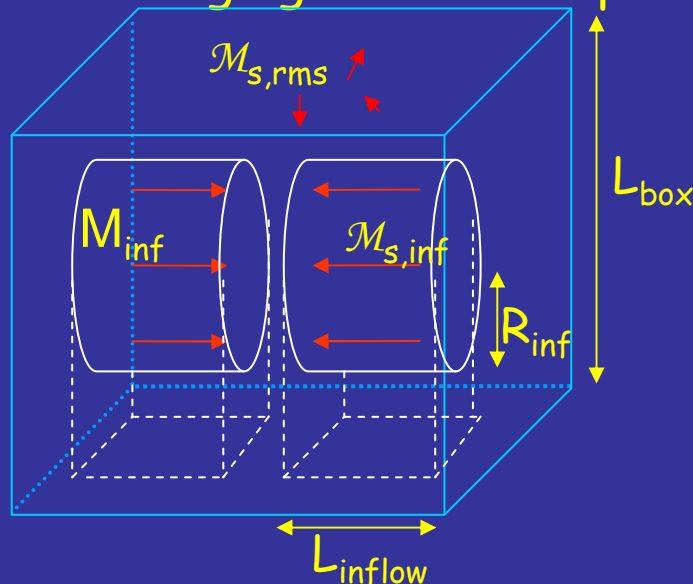
- Use simulations of MC formation by transonic compressions in diffuse WNM (Vázquez-Semadeni et al. 2007, ApJ, 657, 870).



SPH simulation includes **thermal bistability** and self-gravity.

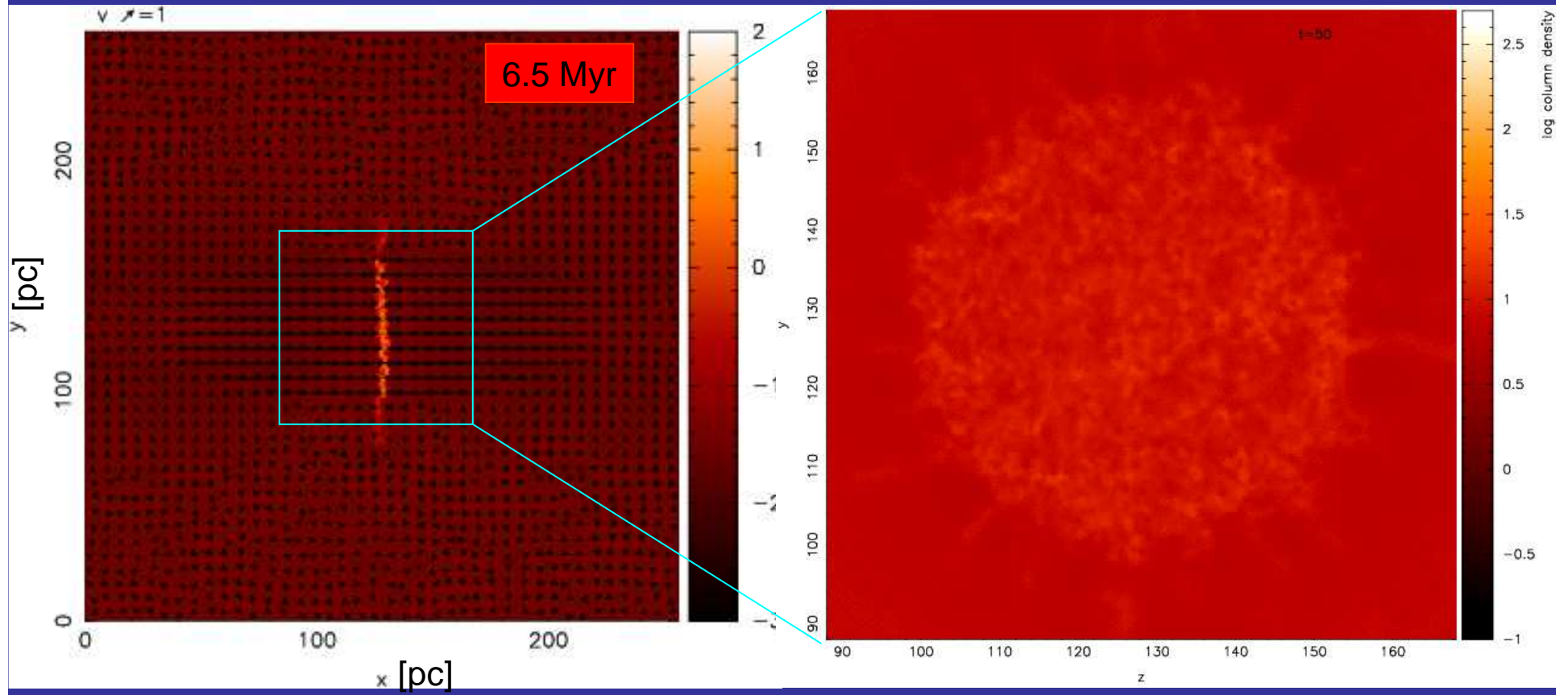
$L = 256 \text{ pc}$
 $\Delta t = 39 \text{ Myr}$
 $\langle n \rangle = 1 \text{ cm}^{-3}$
 $v_{\text{inf}} = 9.2 \text{ km s}^{-1}$
 $T_{\text{ini}} = 5000 \text{ K}$

Converging inflow setup

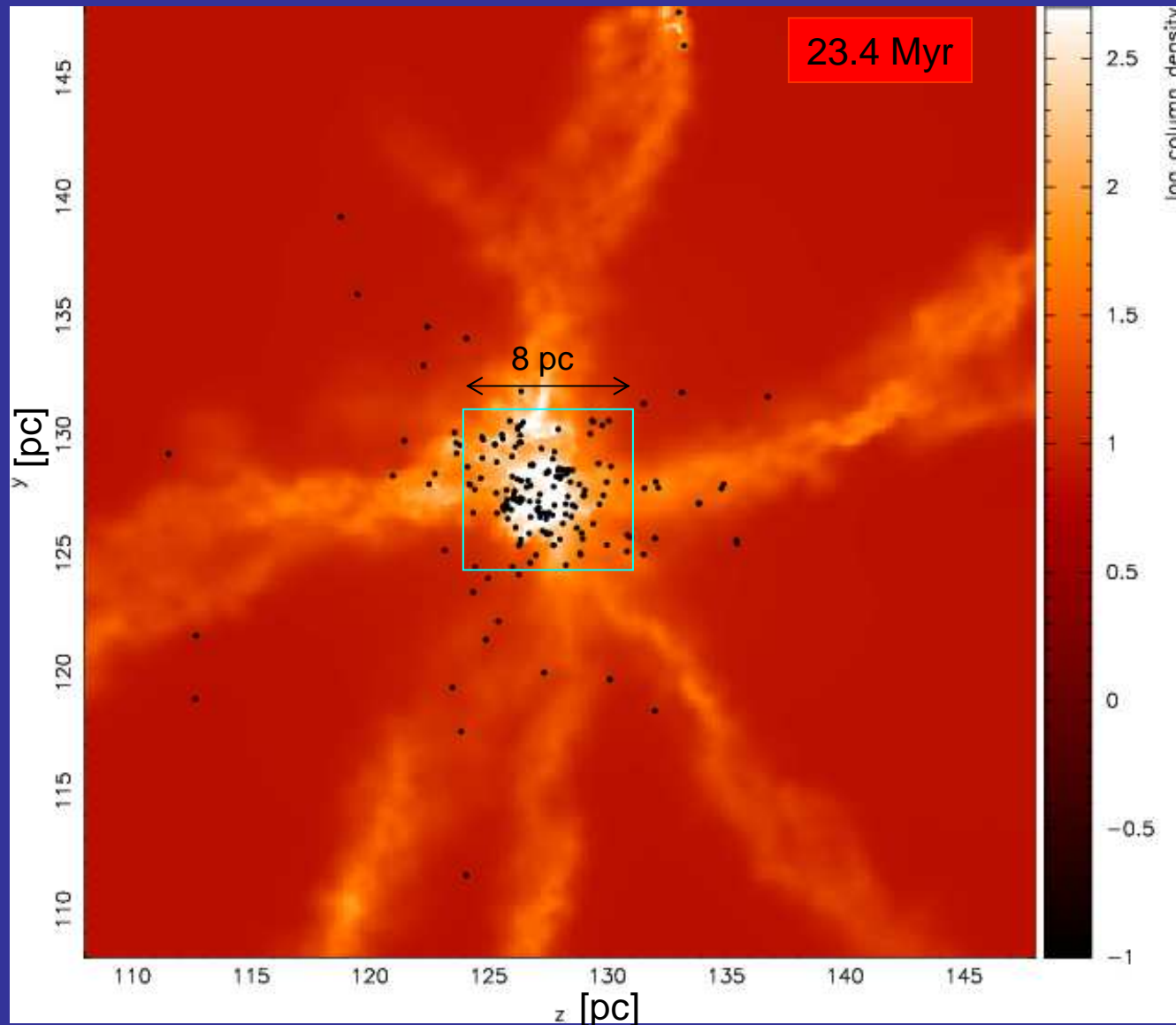


Cloud formation and turbulence generation proceed by TI, KHI, and NTSI as described by VS et al. (2006) and Heitsch et al. (2006).

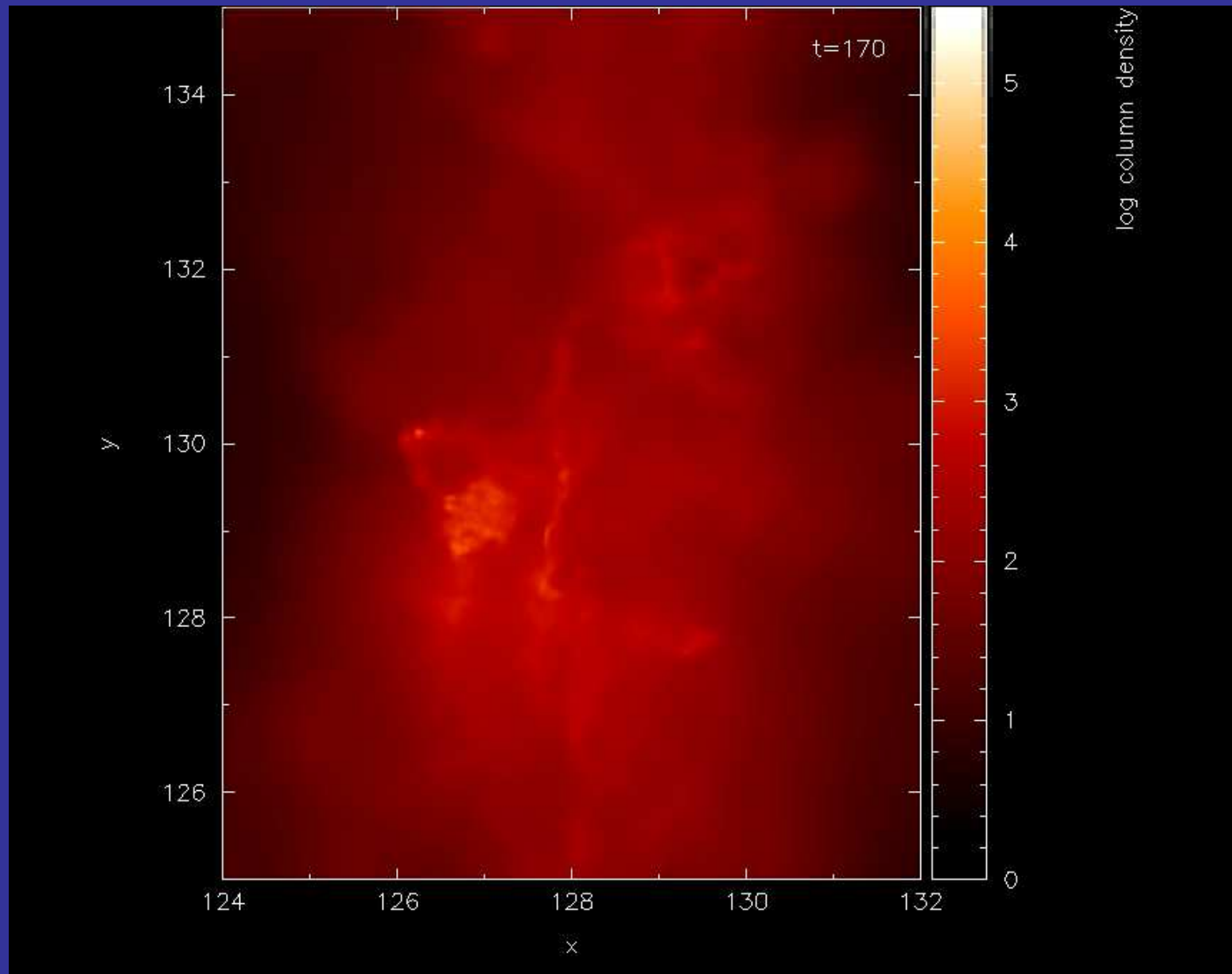
6.5 – 39 Myr



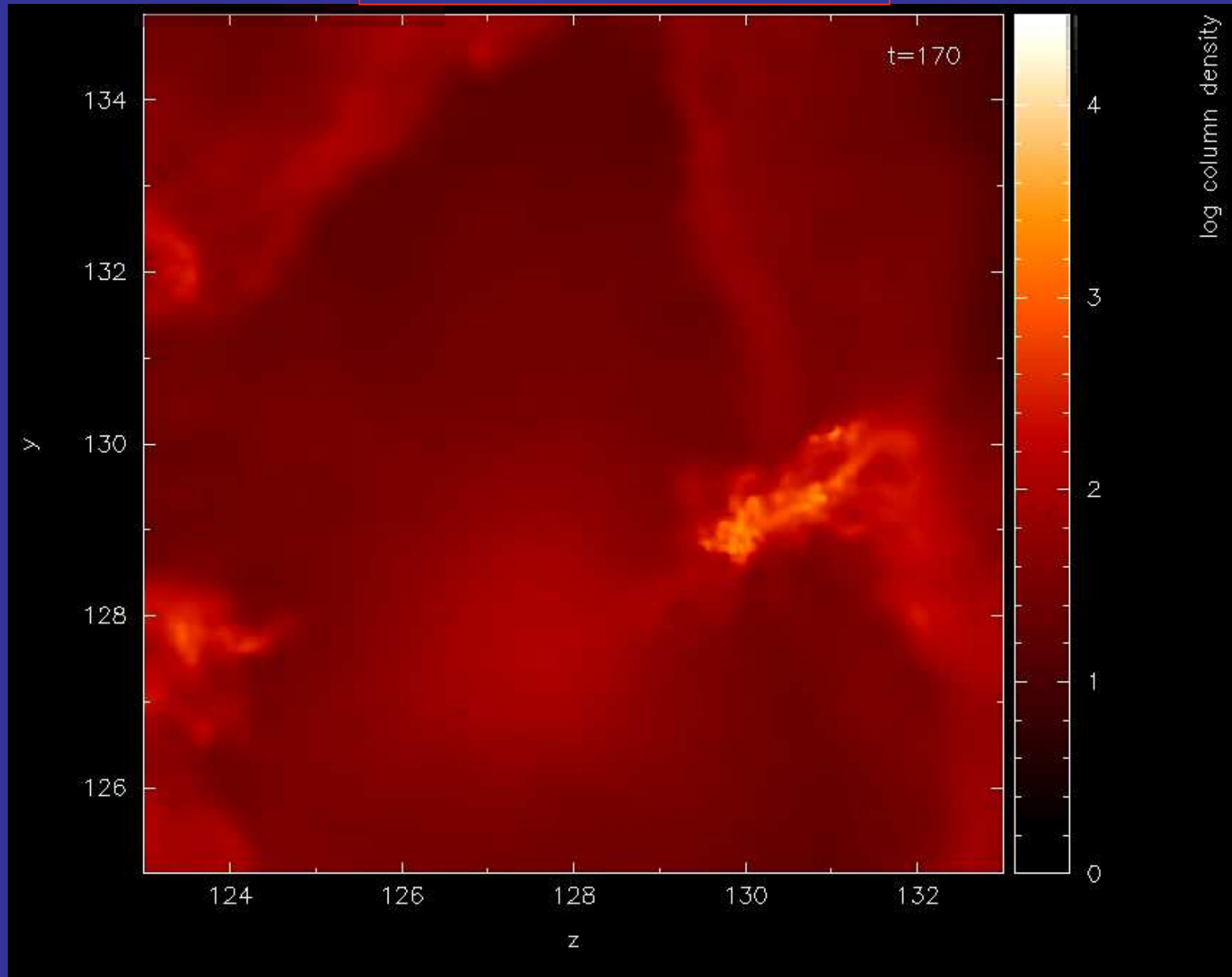
- Focus on time and place of central collision and compare with observations of the high-mass clumps in Cygnus X (Motte et al. 2007, A&A, 476, 1243).

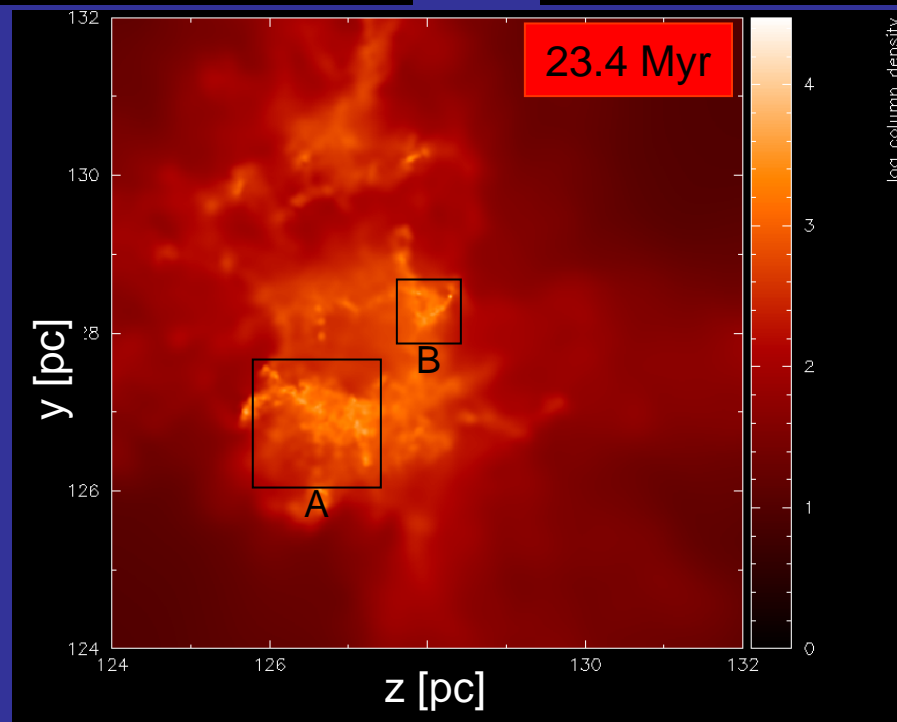
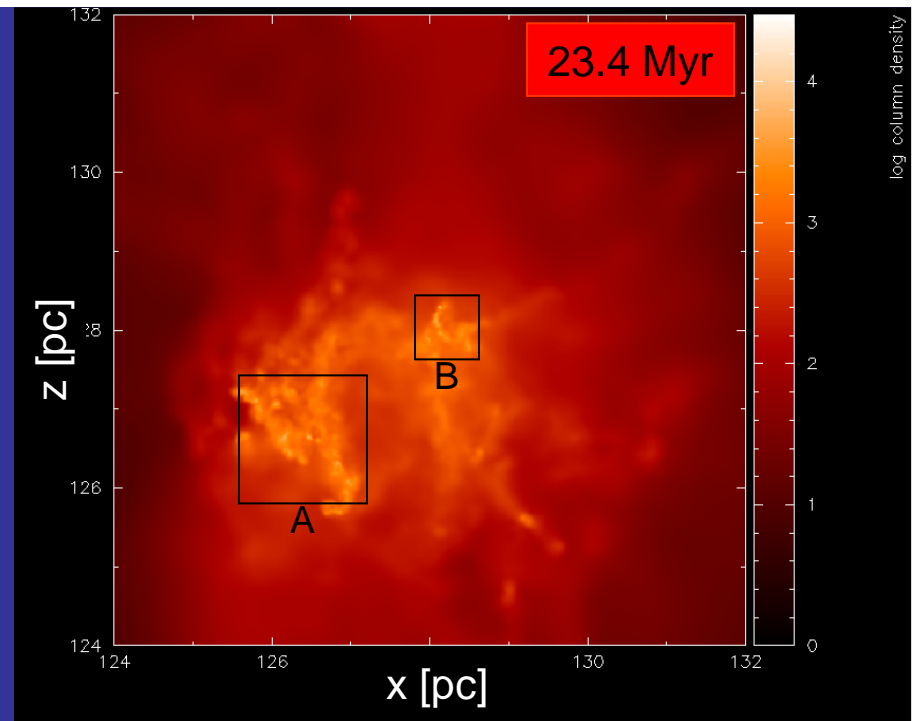
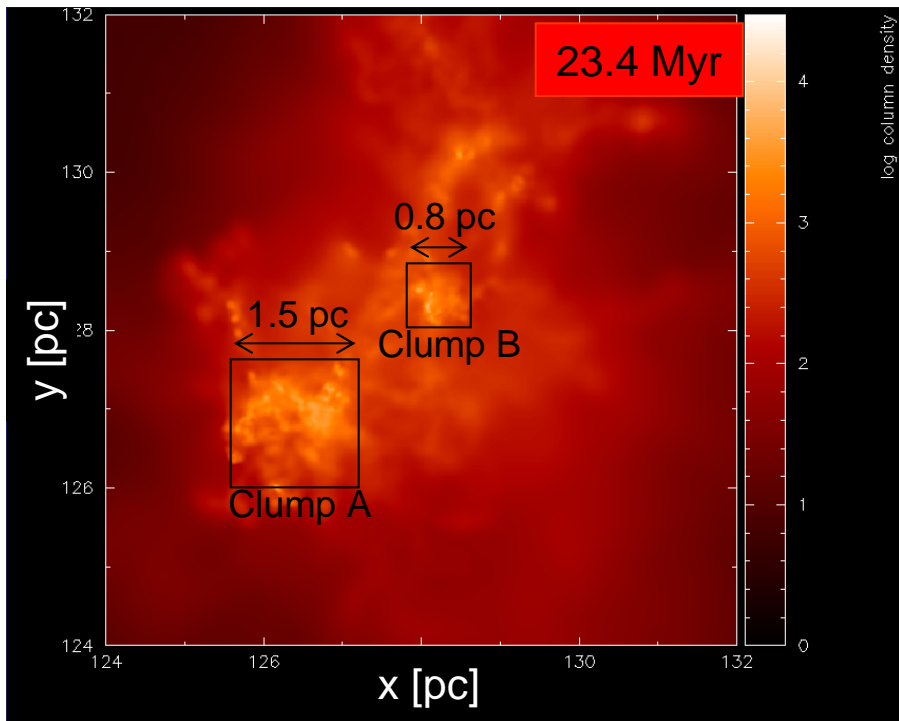


22.1 – 24.7 Myr ($\Delta t = 2.6$ Myr)



22.1 – 24.7 Myr ($\Delta t = 2.6$ Myr)





Central 8 pc
resampled
@ 256^3
(0.03 pc)
resolution.

- **Physical properties:**

- **Whole 8-pc region:**

- $\langle n \rangle = 450 \text{ cm}^{-3}$
- $\sigma_{3D} = 5.0 \text{ km s}^{-1}$
- $M \sim 7000 M_{\text{sun}}$
- Mass accretion rate $\sim 3 \times 10^{-3} M_{\text{sun}} \text{ yr}^{-1}$
- $\sigma_x = 2.3 \text{ km s}^{-1}$; $\sigma_y, \sigma_z \sim 3.1 \text{ km s}^{-1}$

- **Clump A (L = 1.5 pc):**

- $\langle n \rangle = 1.27 \times 10^4 \text{ cm}^{-3}$
- $\sigma_{3D} = 3.6 \text{ km s}^{-1}$
- $M \sim 1400 M_{\text{sun}}$

- **Clump B (L = 0.8 pc):**

- $\langle n \rangle = 1.72 \times 10^4 \text{ cm}^{-3}$
- $\sigma_{3D} = 2.8 \text{ km s}^{-1}$
- $M = 300 M_{\text{sun}}$

“Typical” Motte et al. (2007) clump:
L ~ 0.8 pc
n ~ 7000 cm⁻³

- **High-density cores:** (density threshold criterion, $n > 1, 3, 10, 30 \times 10^4 \text{ cm}^{-3}$, $M > 4 M_{\text{sun}}$).

- Found 38 cores with
 - $n_{\text{max}} \sim 10^{5-6} \text{ cm}^{-3}$.
 - *Lifetimes* $\ll 1.3 \times 10^5 \text{ yr}$ (appear and disappear in $\ll dt$ between frames). Compare to Motte’s estimate: $\sim 10^3 \text{ yr}$.

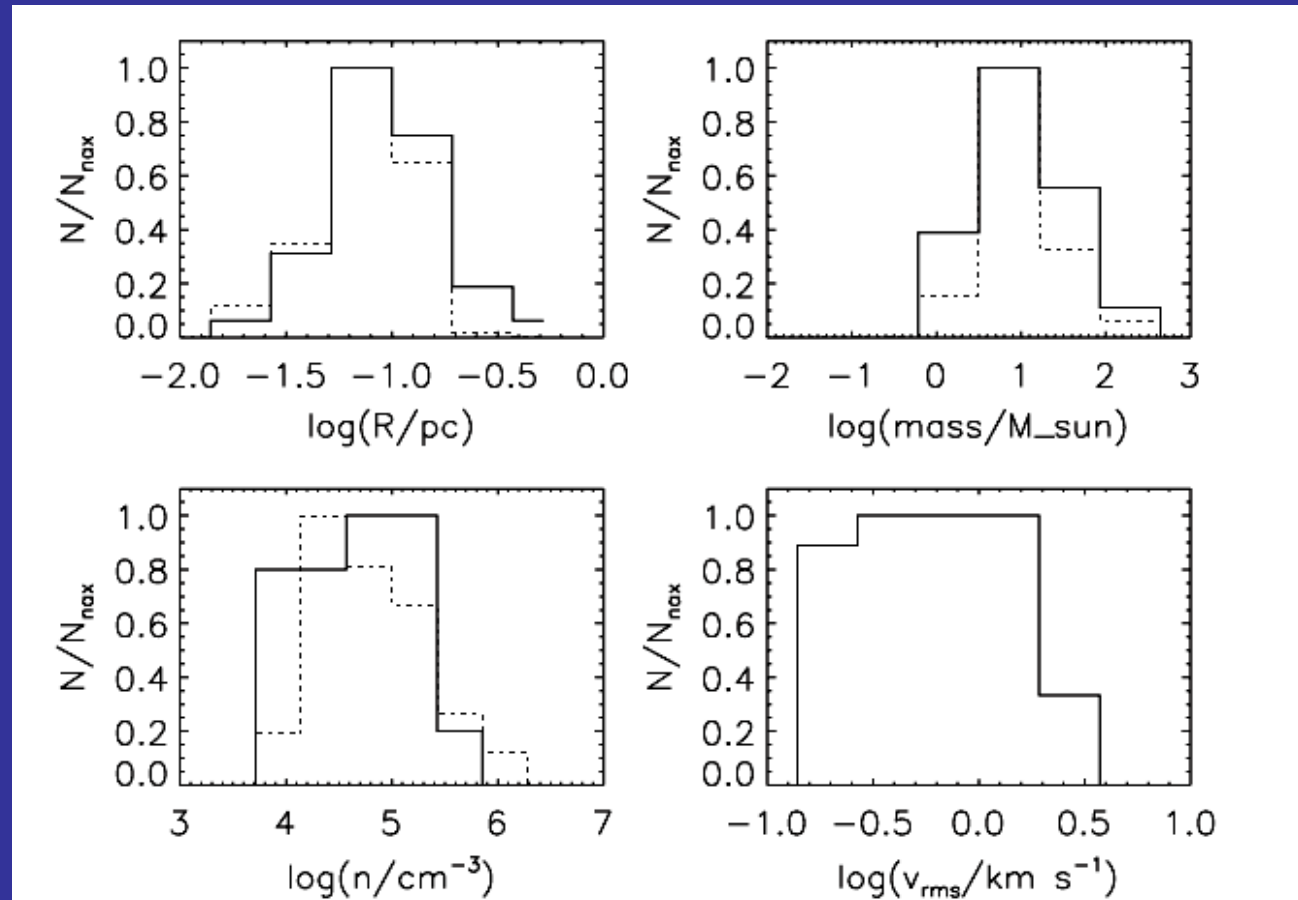
- Core statistics:
 - (Zeroth order confrontation with observations.)

— Simulation

..... Cygnus X-North (129 cores)

(Motte et al. 2007, A&A, 476, 1243;

see also Schneider et al. 2010 arXiv:1003.4198).



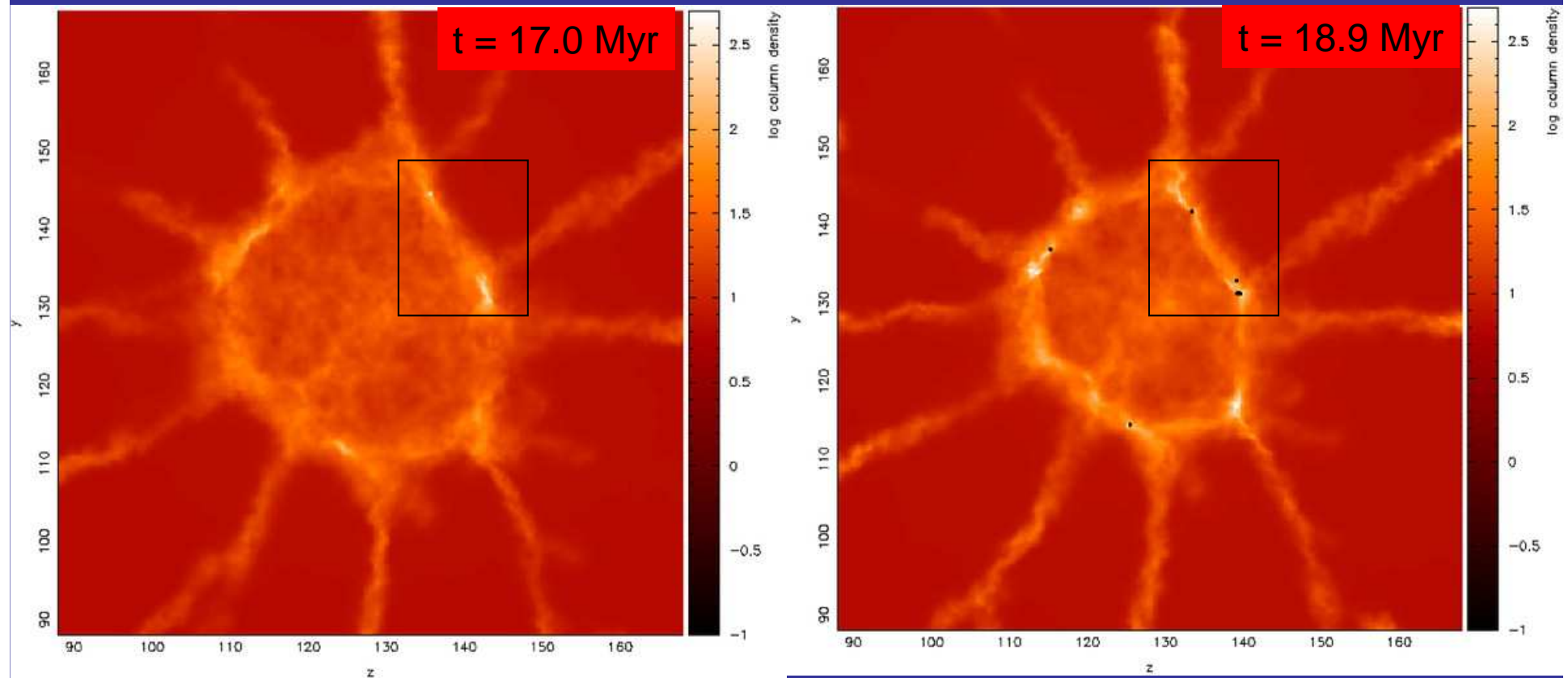
Conclude:

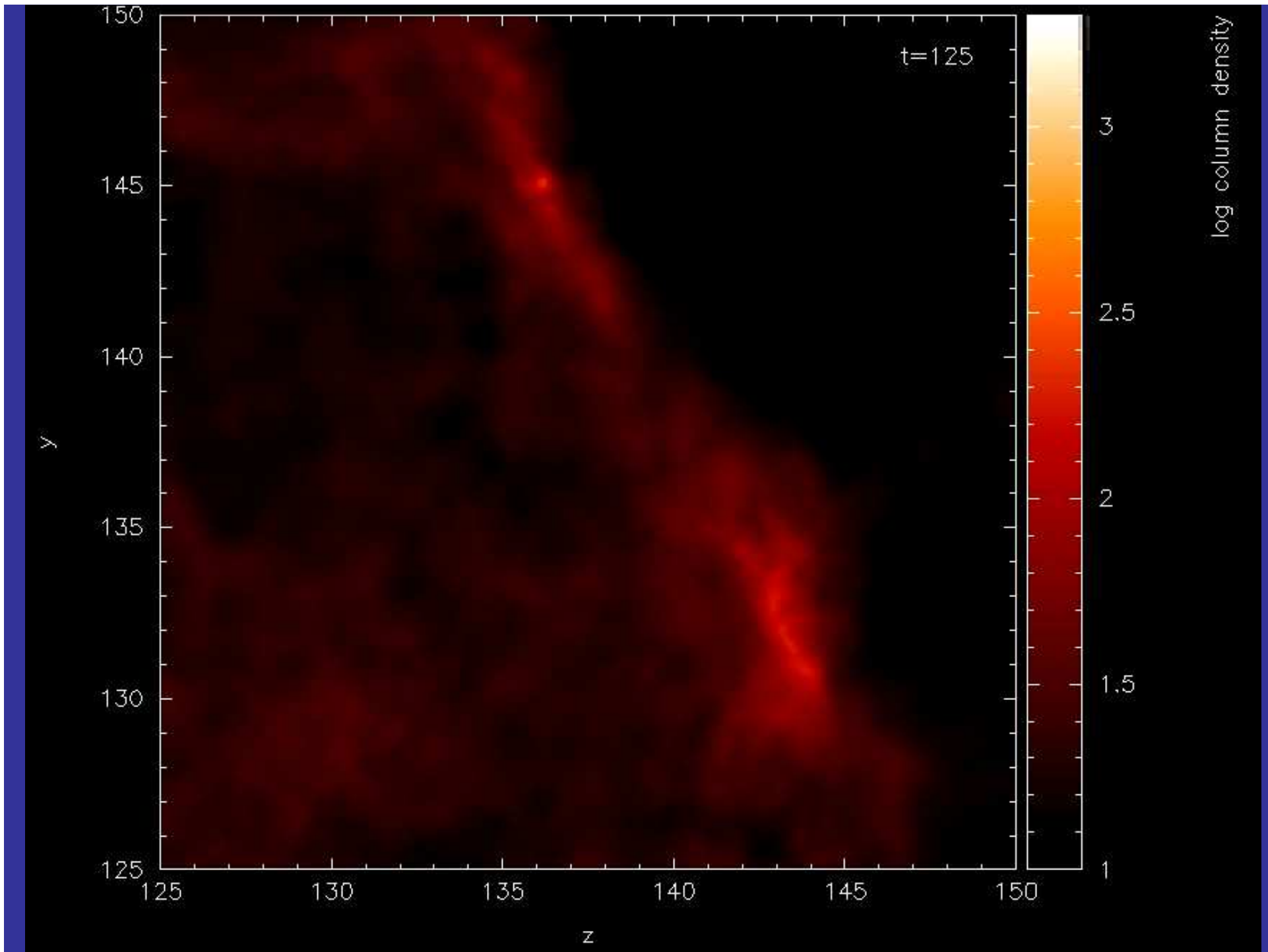
The central region of collapse exhibits similar statistical properties to regions of massive SF.

Note: Velocity field has a significant infall component, not just random turbulence (see also VS et al. 2008, MNRAS, 390, 769).¹

III. LOW-MASS REGIONS

- Now focus on the first star-formation event in the simulation.



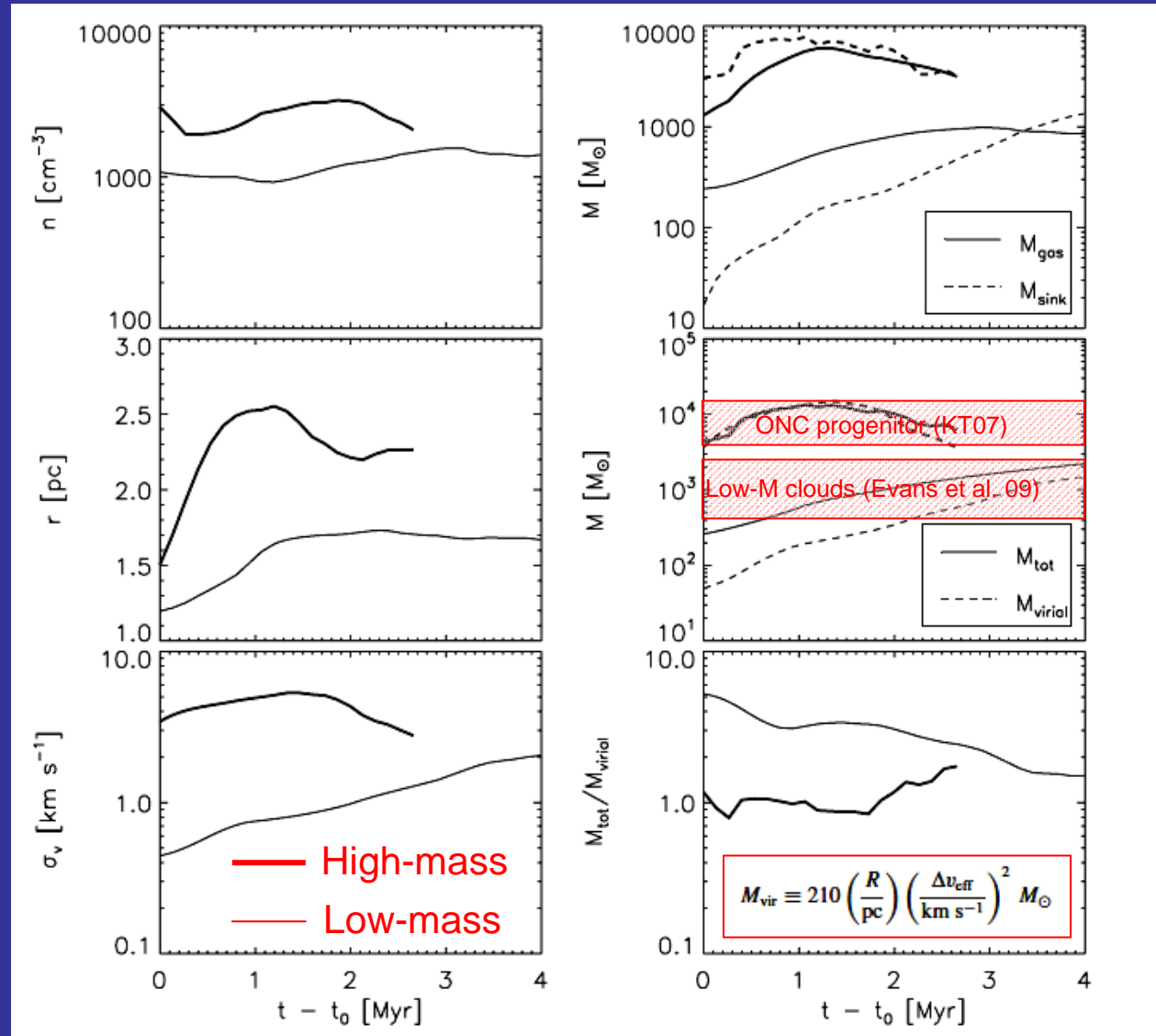


- Comparison of low- and high-mass clouds.

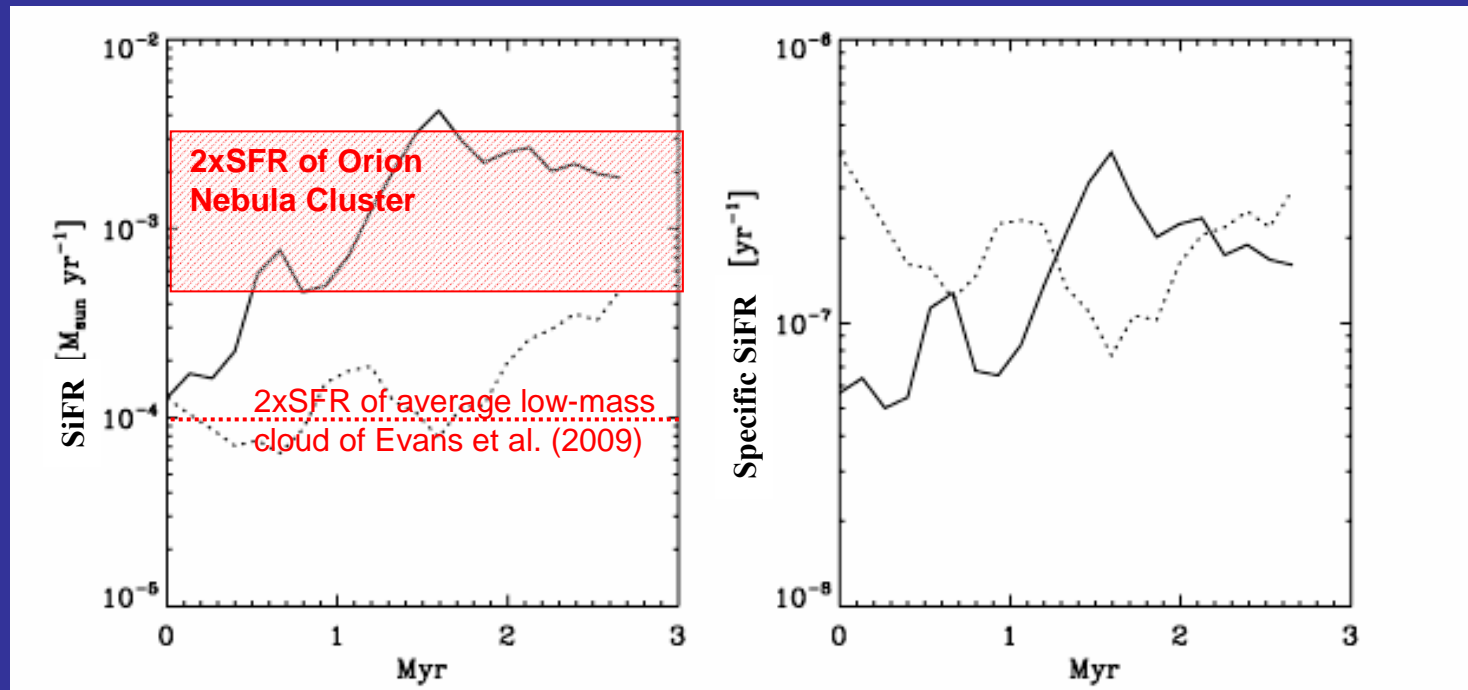
Notes:

- “Clouds” defined by density threshold $n > 500 \text{ cm}^{-3}$.
- Mean density, size, mass and velocity dispersion are all larger in the large-scale collapse region.
- As clouds become increasingly dominated by gravity,

$$\frac{M}{M_{\text{vir}}} \rightarrow 1.$$



- Star formation rates



Notes:

1. SFR estimates for the Orion Nebula Cluster (ONC) from [Krumholz & Tan \(2007\)](#) (high) and [VS et al. \(2009\)](#) (low).
2. Rates in simulation are sink formation rates (SiRF). Assuming SFE $\sim 30 - 50\%$ within sinks suggests $\text{SFR} \sim 0.3 - 0.5 \text{ SiRF}$.
3. Mass depletion times in both clouds $\sim 10 \text{ Myr}$.

- However, **for the high-mass cloud:**

Define a “cluster-forming clump” by $n > 10^4 \text{ cm}^{-3} \rightarrow t_{\text{ff}} \sim 0.3 \text{ Myr}$
@ $T = 10\text{K}$ (threshold contains all SF in the cloud). Then

$$SFE_{\text{ff}} \equiv \frac{M_*(t_{\text{ff}})}{M_{\text{cl}}(t_{\text{ff}}) + M_*(t_{\text{ff}})} = \frac{\langle \text{SFR} \rangle t_{\text{ff}}}{\langle M_{\text{tot}} \rangle} \approx \frac{(500 - 3000 M_{\text{sun}} \text{Myr}^{-1})(0.3 \text{Myr})}{5000 M_{\text{sun}}} \approx 0.01 - 0.06$$

Consistent with SFE_{ff} of cluster-forming clumps, even though the clump is in gravitational collapse.

No need for “support” nor equilibrium.

However, final SFE of cloud too large if process not truncated by feedback.

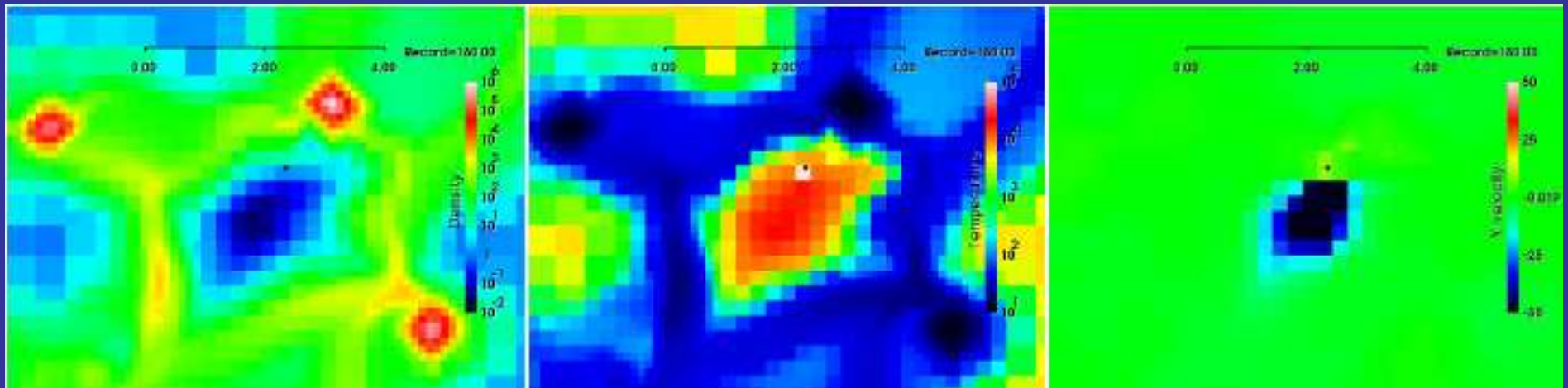
IV. EFFECT OF FEEDBACK AND INITIAL CONDITIONS

- Numerical model:
 - N-body + AMR hydrodynamics code ART (Kravtsov et al. 1997; Kravtsov 2003).
 - 256-pc box.
 - 4 refinement levels. Equivalent resolution 2048^3 .
 - 0.125 pc resolution.
 - Same colliding-flow setup.
 - Stellar particle formation by density threshold criterion.
 - $n_{\text{SF}} = 4 \times 10^6 \text{ cm}^{-3}$.
 - $M_{\text{part}} \sim \frac{1}{2} M_{\text{cell}} \sim 120 M_{\text{sun}} \rightarrow 1 \text{ particle} = 1 \text{ small cluster}$.
 - Cooling function from Koyama & Inutsuka (2002).

- Numerical model (cont'd)

- B6-star ionization-like heating by stellar particles:

- Deposited in cell containing stellar particle during 10 Myr.
 - Heating rate taken as free parameter, adjusted to achieve “realistic” HII regions:



Density

Temperature

Velocity

- *Caveat:* Same feedback rate in all cases:
 - Overestimate effect in low-mass clouds, underestimate in high-mass ones.

- Four simulations:

Large-amplitude initial fluctuations

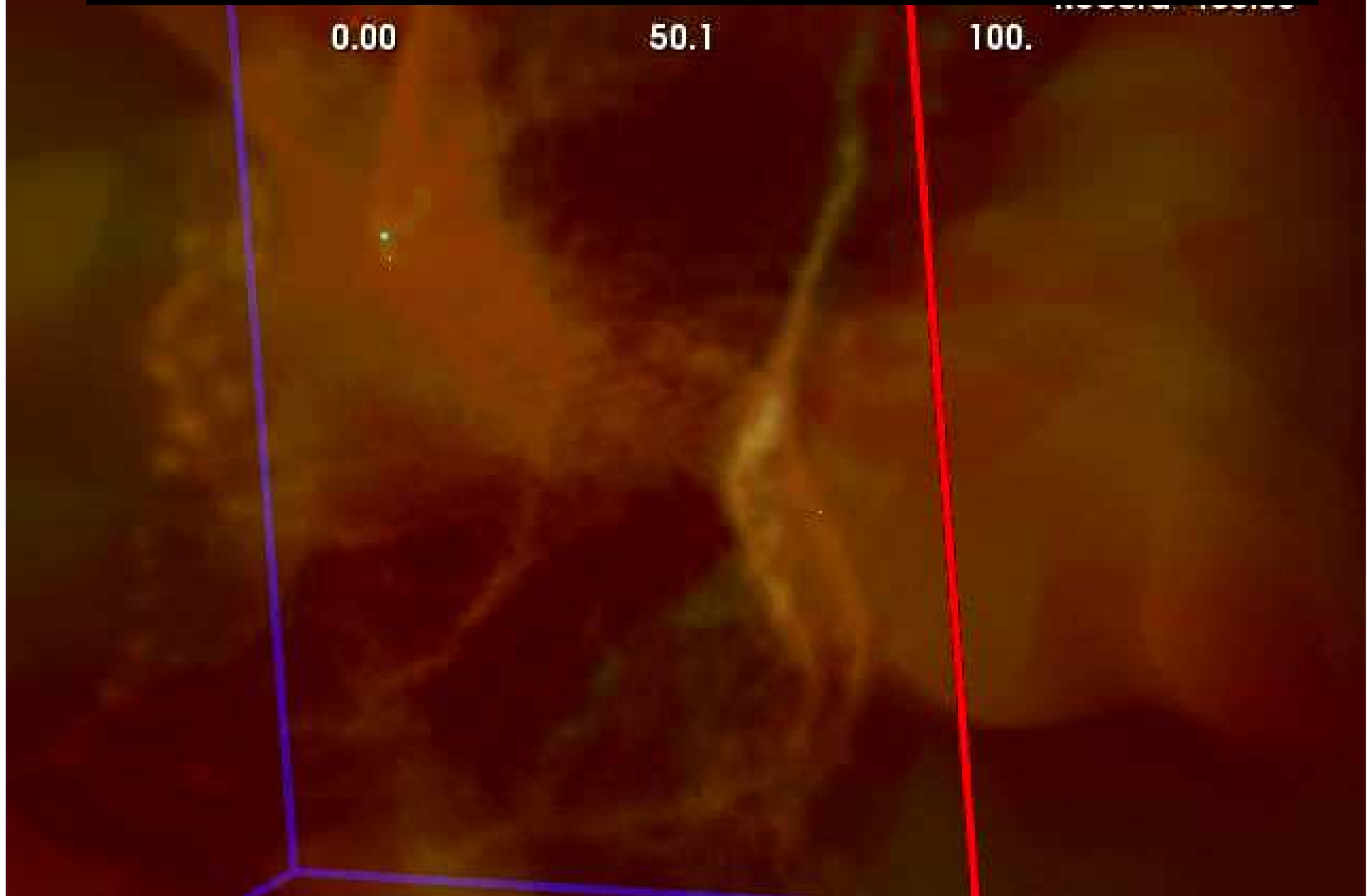
Small-amplitude initial fluctuations

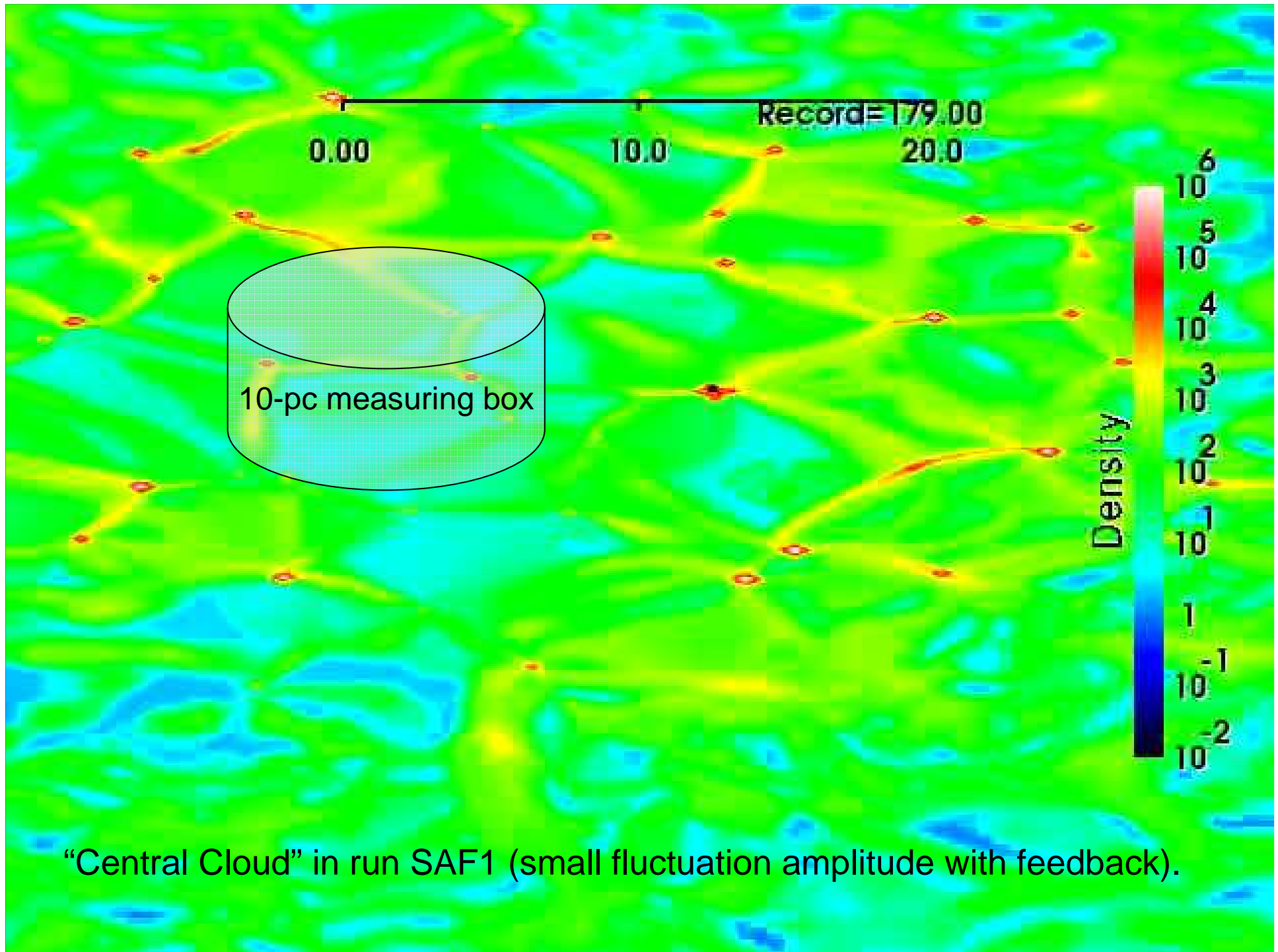
Table 1: RUN PARAMETERS

Run name	v_{rms} [km s ⁻¹]	Feedback
LAF0	1.7	off
LAF1	1.7	on
SAF0	0.1	off
SAF1	0.1	on

- ...applied at scales $\sim \frac{1}{2}$ the diameter of the inflows.
- The initial convergent flow may be considered a large-scale fluctuation.

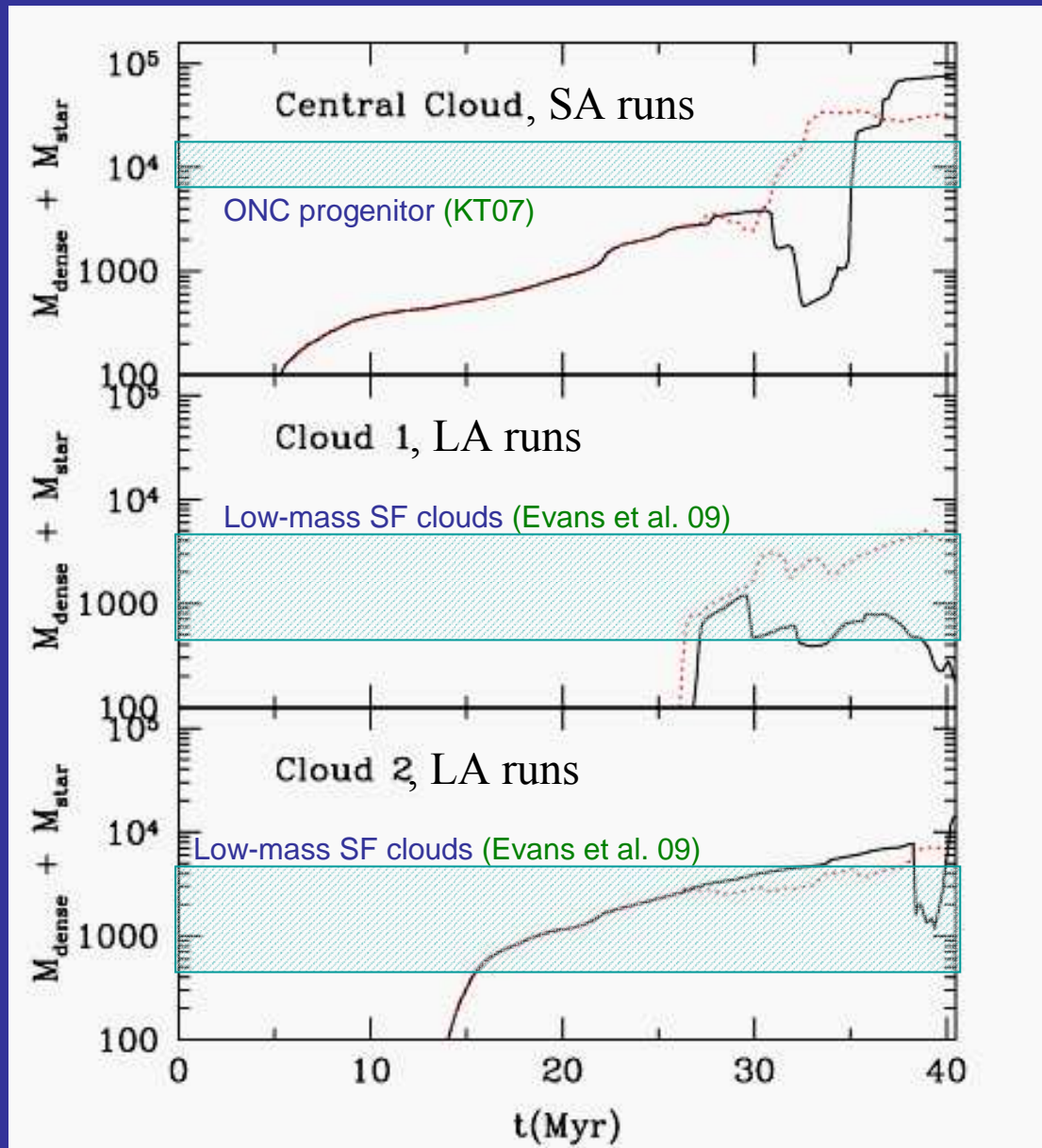
- Run LAF1 (Large-amplitude fluctuations with feedback).
Clouds 1 and 2.





“Central Cloud” in run SAF1 (small fluctuation amplitude with feedback).

Masses:



..... Feedback off
— Feedback on

Clouds somewhat more massive than previous study, so not directly comparable.

- **Results:**

1. More massive clouds are more robust against dispersal by stellar feedback (see also Krumholz, Matzner & McKee 2006).

Massive cloud is not kept near virial equilibrium...

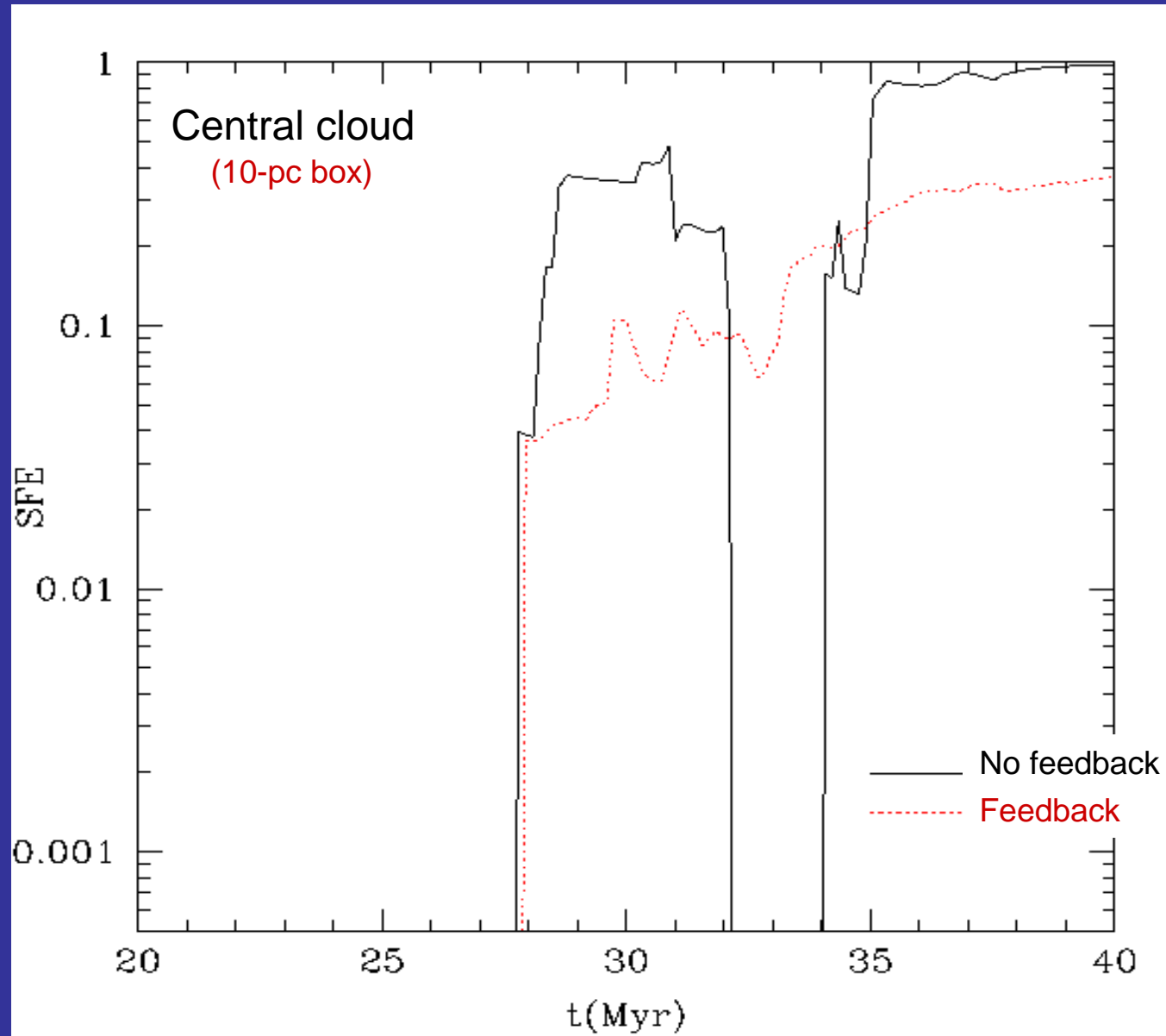
... nor dispersed!

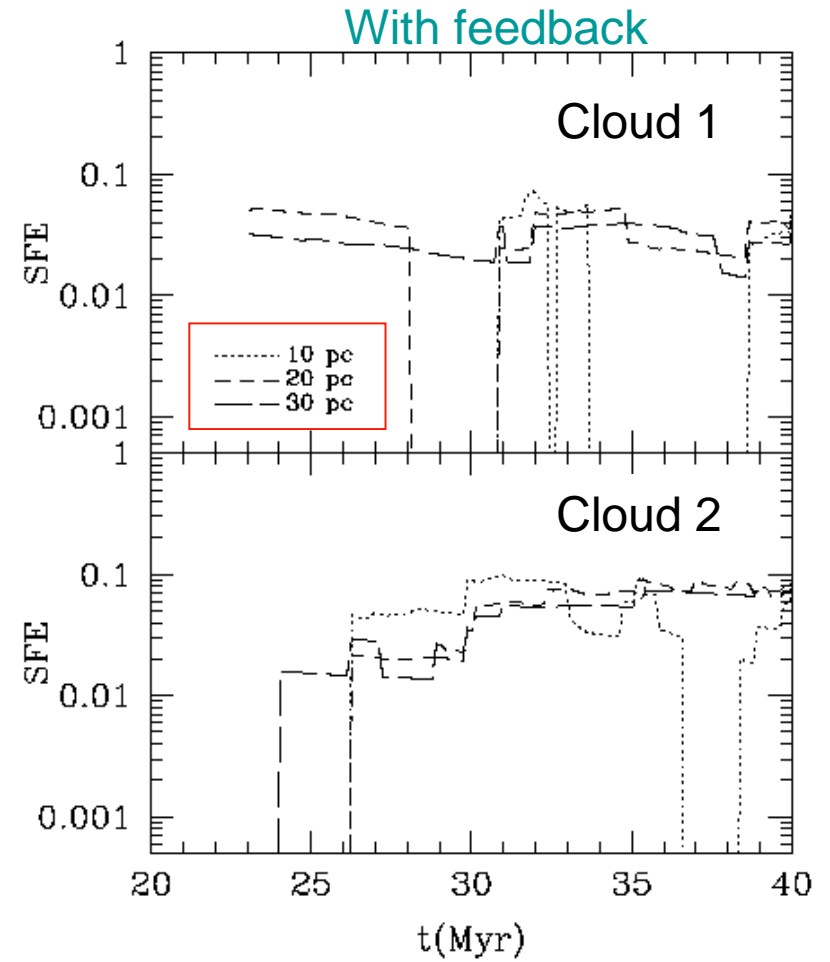
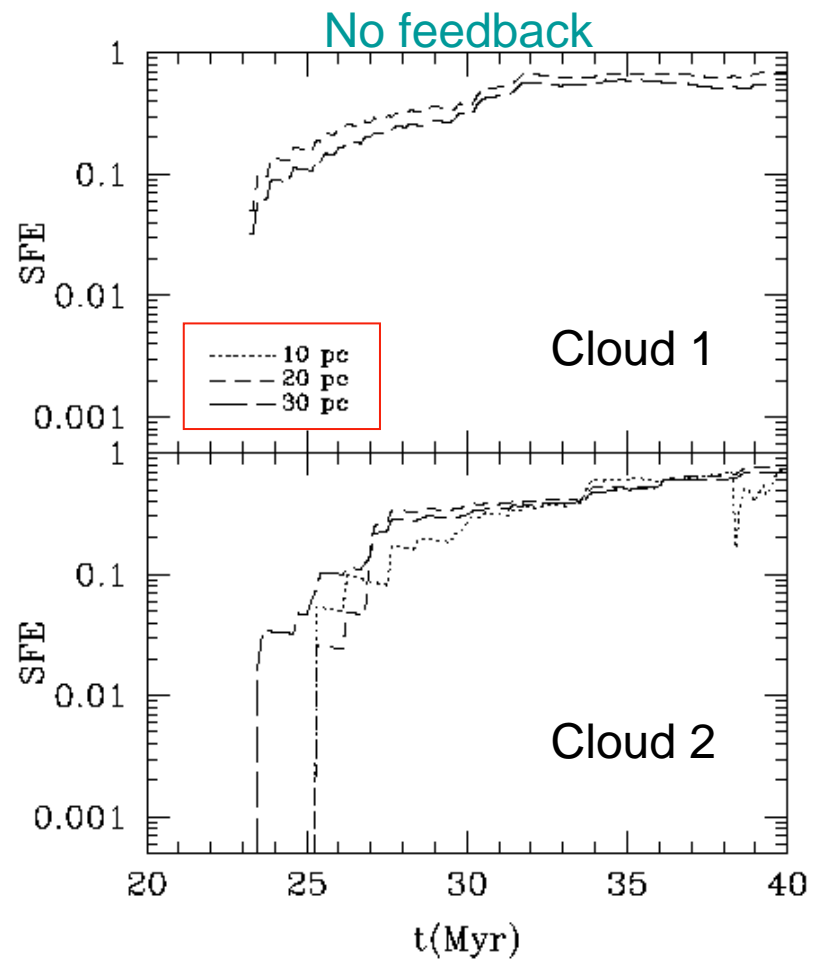
Instead, *accretion approximately balances gas consumption by SF and dispersal by feedback.*

The clouds are continually processing material

- Similar to a candle's flame.
- Due to large-scale potential well.

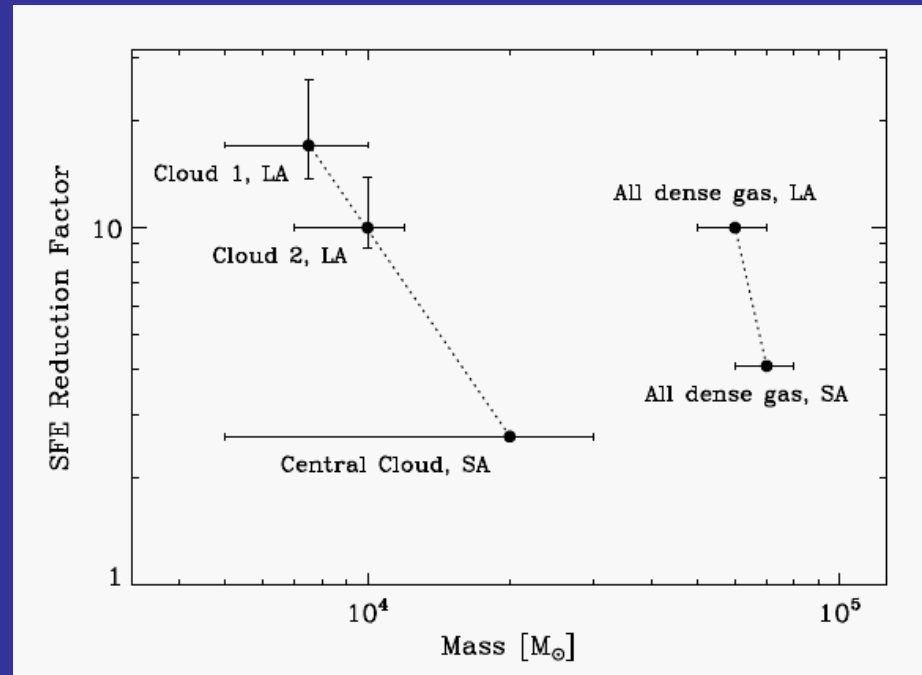
2. SFE is strongly reduced with feedback, *and maintained at low values.*





- Reduction of SFE due to inhibited conversion of dense gas to stars by feedback.
 - Cloud masses not very different upon inclusion of feedback.
- Slow variation of SFE over time apparently due to accretion replenishing the gas mass while SF proceeds.

3. Factor by which feedback reduces SFR depends on the cloud mass (at roughly the same size) involved in coherent collapse.



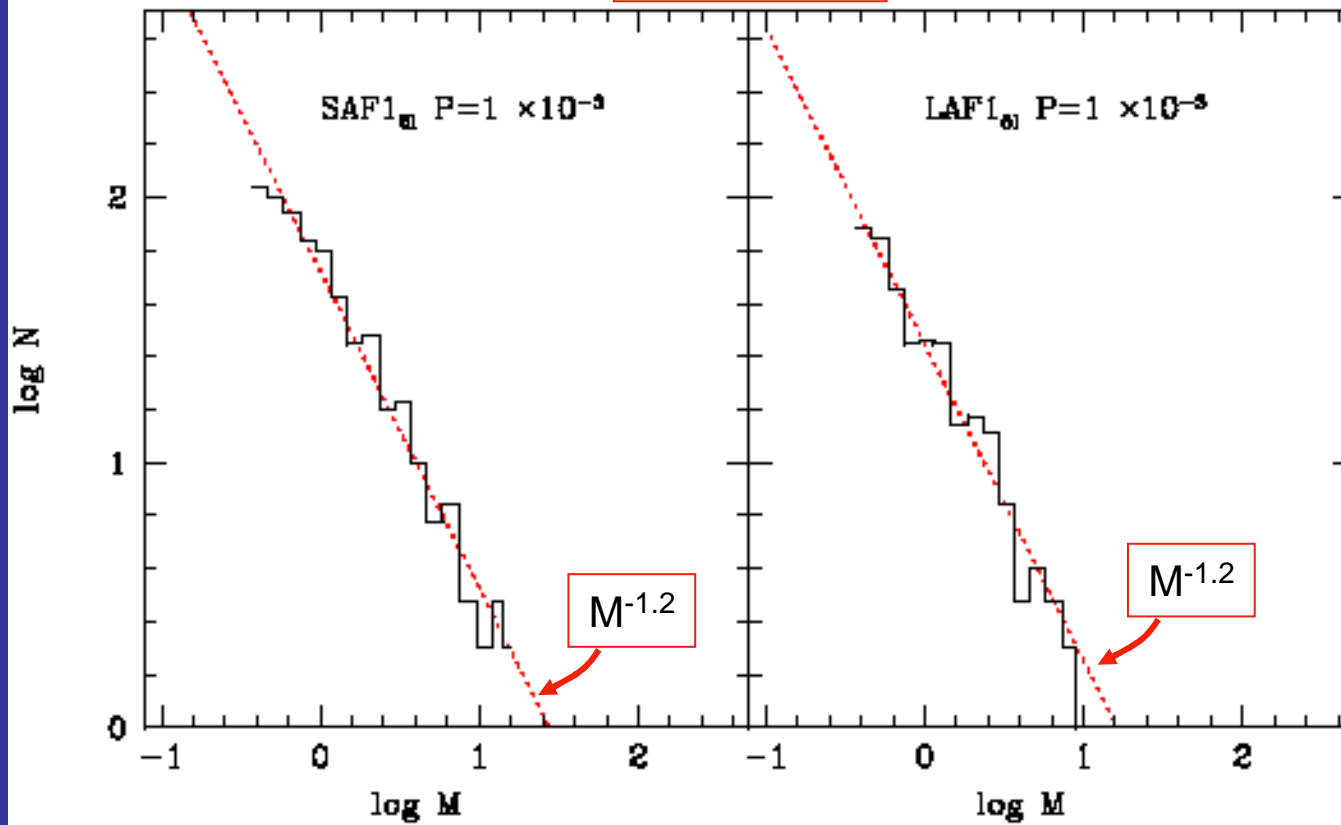
- Apparently due to short-range effect of feedback vs. long-range nature of gravity.
 - The more extended the infall motions, the less effective the feedback in disrupting them.
 - Effect probably exaggerated by single feedback-star mass in simulations.

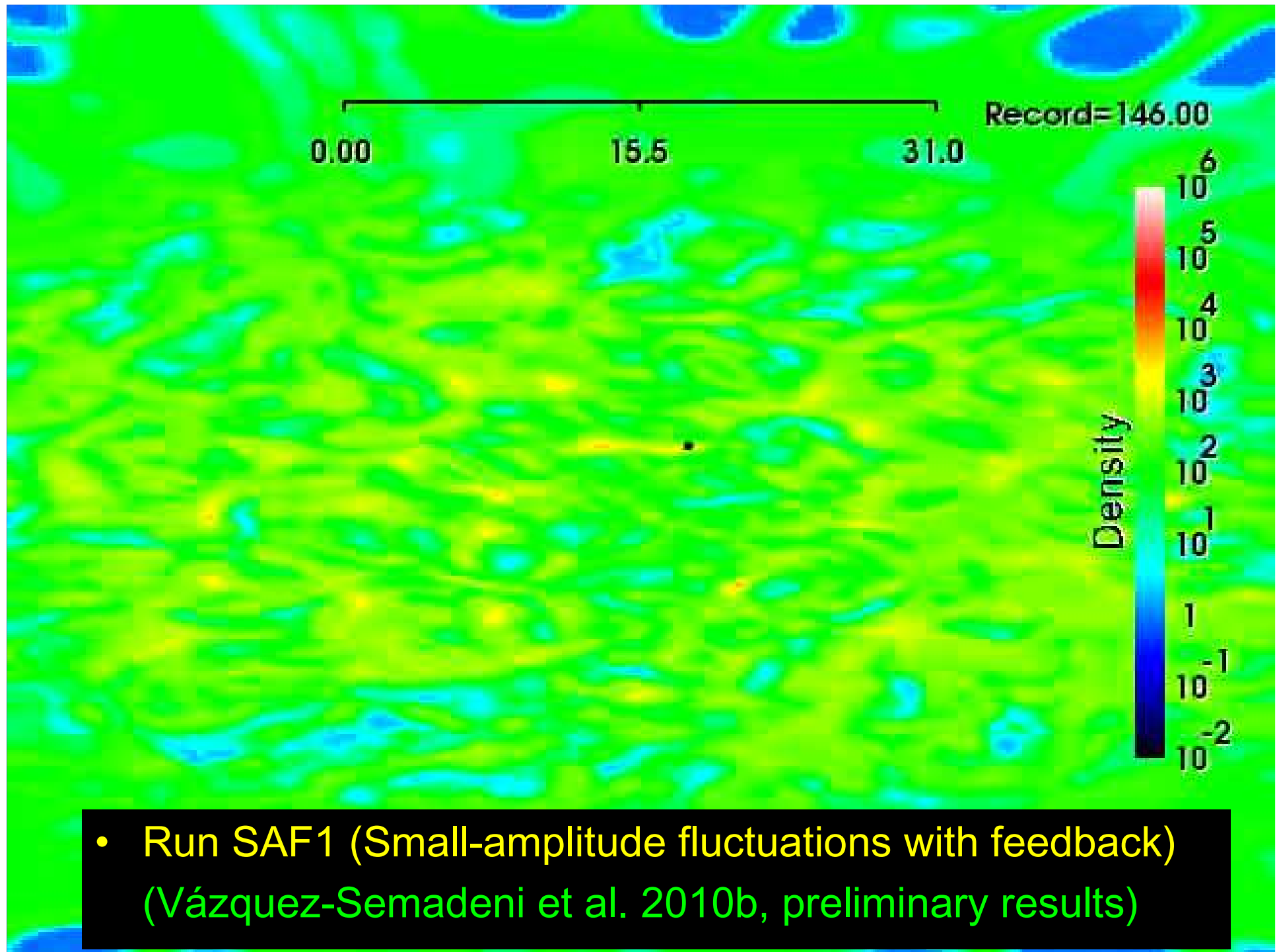
- Improvements:

- Work in progress: consideration of a range of stellar masses and corresponding feedback strengths (Vázquez-Semadeni et al. 2010b, in prep.).
 - Each stellar particle is a star.
 - A power-law IMF: $dN/dM \sim M^{-1.2}$ (input, not prediction).
 - Results from forming stars with small probability (0.001) when density threshold is reached.
 - Preliminary feedback recipe:
 - Piecewise power-law dependence of stellar heating on mass:

$$L = 3.2 \times 10^{37} \left(\frac{M}{9M_{\text{sun}}} \right)^{\beta} \text{ erg s}^{-1} \quad \longrightarrow \quad \text{Upper limit}$$
$$\beta = \begin{cases} 3.8 & \text{for } M > 9M_{\text{sun}} \\ 6.7 & \text{for } M < 9M_{\text{sun}} \end{cases}$$

Stellar IMF





- Even the upper-limit feedback strength cannot suppress global infall.

0.00 25.9 Record=145.00
51.9

“Cloud 2” in run LAF1 (Large fluctuation amplitude with feedback).

- Suggested conclusions:

- *Physical properties of low- and high-mass star-forming regions may arise simply from gravitational contraction.*
- The coherence and scale of the initial fluctuations in the WNM determine whether the star-forming regions that form are of high- or low-mass.
 - Large-scale coherent collapse → Massive star-forming regions.
 - Small-scale coherent collapse → Low-mass regions.
 - Gravitational contraction gives $M/M_{\text{vir}} \sim 1$.
- SFRs of high- and low-mass regions (without feedback) within factors of a few of observations.
- With feedback:
 - SFR further reduced by factors 3 (high-mass) – 10 (low mass).
 - SFEs remains relatively constant in time.
 - Feedback acts at small scales, gravitational accretion at large scales.
 - » Feedback cannot oppose large-scale accretion.
 - » Effect more important in more massive clouds.
- Work in progress:
 - Feedback dependent on stellar mass.
 - Magnetic fields and ambipolar diffusion (see Robi Banerjee's talk).

The End